



Design, synthesis and biological evaluation of novel pteridinone derivatives possessing a hydrazone moiety as potent PLK1 inhibitors

Zhiwei Li^a, Le Xu^a, Liangyu Zhu^a, Yanfang Zhao^a, Tao Hu^b, Bixi Yin^b, Yajing Liu^{a,*}, Yunlei Hou^{a,b,*}

^a School of Pharmaceutical Engineering, Shenyang Pharmaceutical University, 103 Wenhua Road, Shenhe District, Shenyang 110016, China

^b Yangtze River Pharmaceutical Group Pharmaceutical Co., Ltd, 1 South Yangtze River Road Taizhou, Jiangsu 225321, China

ARTICLE INFO

Keywords:

PLK1
Pteridinone derivatives
Anti-cancer

ABSTRACT

A series of novel pteridinone derivatives possessing a hydrazone moiety were designed, synthesized and evaluated for their biological activity. Most of the synthesized compounds demonstrated moderate to excellent activity against A549, HCT116 and PC-3 cancer cell lines. In particular, compound L₁₉ exhibited the most potent antiproliferative effects on three cell lines with IC₅₀ values of 3.23 μM, 4.36 μM and 8.20 μM, respectively. In kinase assays, the compound L₁₉ also showed potent inhibition activity toward PLK1 with % inhibition values of 75.1. Further mechanism studies revealed that compound L₁₉ significantly inhibited proliferation of HCT-116 cell lines, induced a great decrease in mitochondrial membrane potential resulting in apoptosis of cancer cells, inhibited the migration of tumor cells, and arrested G1 phase of HCT116 cells.

Cancer, manifesting through abnormal regulation of multiple signaling pathways, remains the second leading disease and one of the major public health problems.^{1,2} To overcome cancer, the conventional strategy was to design and synthesize new antitumor drugs that inhibited at least one protein involved in these pathways.³ With the advancement of scientific and technological methods, the secrets of malignant proliferation of tumor cells have gradually been discovered, such as the disorder of cell signaling pathways and uncontrolled cell proliferation.⁴ Research on anti-tumor drugs targeting key factors that regulate the cell cycle has attracted increasing attention from researchers.

Polo-like kinases (PLKs), a serine–threonine kinase, have five family members (PLK1–5) which play a key role in mitosis and have been proven to be necessary for centrosome maturation and bipolar spindle formation.^{5–7} PLK1 is the most widely studied of all PLK family members, the molecular mechanism responsible for reciprocal activation between PLK1 and MYCN (v-myc myelocytomatosis viral related oncogene, neuroblastoma derived) have been identified.⁸ The over-expression of PLK1 have been found in many different tumor types, including lung cancer, colon cancer, prostate cancer, ovarian cancer, breast cancer, head, neck squamous cells cancer and melanoma.⁹ Due to its essential role in cell proliferation, PLK1 have been identified as a broad-spectrum anticancer target.

In recent years, a variety of effective PLK1 small molecule inhibitors

have been developed, such as BI-2536, BI-6727 (volasertib), NMS-P937, GSK461364 and TAK960 have advanced clinical trials and shown encouraging anticancer effects in many kinds of tumors^{10–14} (Fig. 1). Among these promising anticancer agents, BI-2536 has reached phase II trials and showed inspiring results.¹⁰

The co-crystal structure of the PLK1 catalytic domain in complex with BI-2536 revealed that BI-2536 aminopyrimidine moiety binded to hinge region Cys 133 via two hydrogen bonds and pteridinone carbonyl formed two water-mediated hydrogen bonds with the side chain of Lys 82 and the main chain NH of Asp 194, respectively. Thus the dihydropteridinone framework played key roles in the interaction with PLK1 kinase¹⁵ (Fig. 2). As a continuation of our previous study of dihydropteridinone PLK1 kinase inhibitors,¹⁶ we modified the framework of BI-2536 by replacing the 7-position ethyl group with a hydrogen-bond acceptor carbonyl group in order to form a hydrogen bond with the protein (Fig. 3).

In addition, hydrazone derivatives showed a broad spectrum of biological activities in the medical field, such as antimicrobial,¹⁷ anti-tuberculosis¹⁸ and antitumor activities.¹⁹ Presumably, the bioactivity based on hydrazone moiety was due to the hydrazone's easy to bind to molecular targets as a hydrogen bond donor or acceptor. In addition, the functional group can also give a certain degree of flexibility to the chemical structure.^{20,21} Due to its beneficial properties, we are motivated to combine this moiety with the dihydropteridinone skeleton to

* Corresponding author at: School of Pharmaceutical Engineering, Shenyang Pharmaceutical University, 103 Wenhua Road, Shenhe District, Shenyang 110016, China (Y. Hou).

E-mail addresses: lyjpharm@126.com (Y. Liu), hoyunlei901202@163.com (Y. Hou).

<https://doi.org/10.1016/j.bmcl.2020.127329>

Received 15 April 2020; Received in revised form 3 June 2020; Accepted 4 June 2020

Available online 08 June 2020

0960-894X/ © 2020 Elsevier Ltd. All rights reserved.

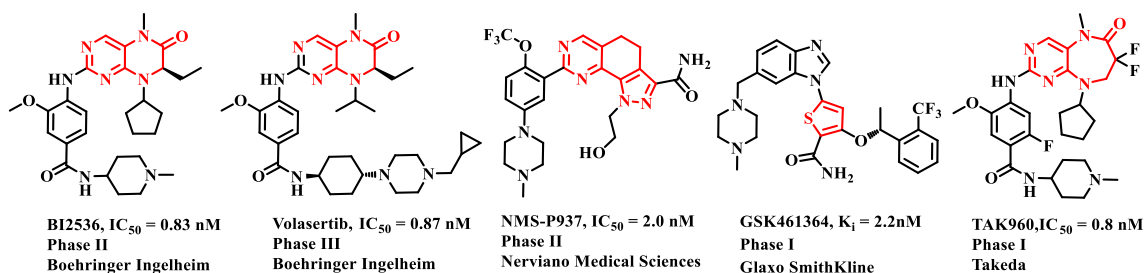


Fig. 1. Structures of PLK1 inhibitors in clinical trials.

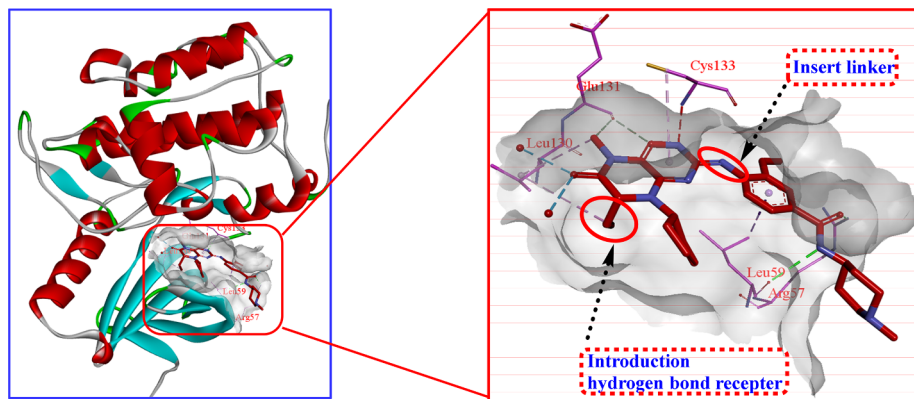


Fig. 2. Crystal structure of BI-2536 bound to PLK1 (PDB ID: 2RKU).

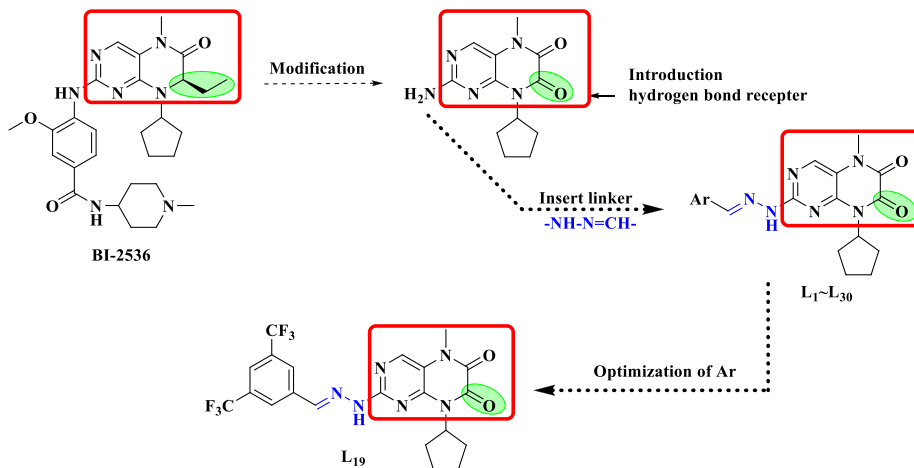
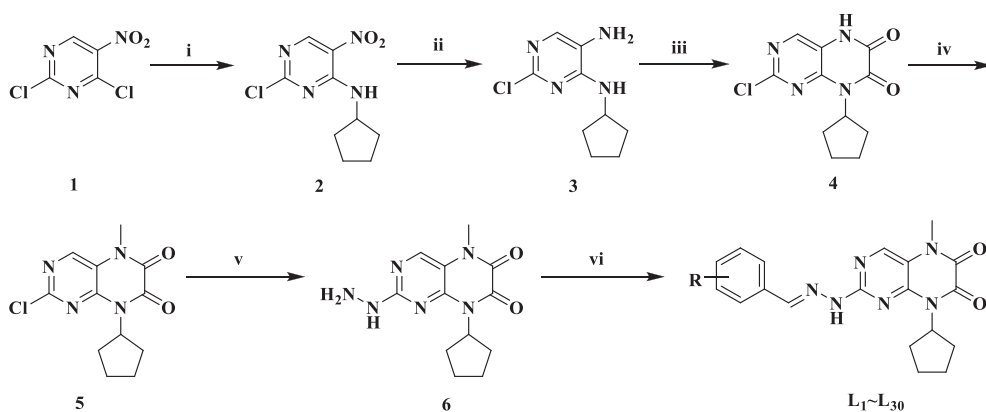


Fig. 3. Design strategy for the target compounds.

design novel PLK1 kinase inhibitors (L_1 – L_{30}) (Fig.3). All compounds were subsequently assayed for *in vitro* anti-proliferative activities against three cancer cell lines A549, HCT116 and PC-3. According to the antiproliferative results, an effective compound L_{19} was selected for further *in vitro* enzyme inhibition studies. To elucidate the primary main mechanism, L_{19} was examined by *in vitro* the migration, apoptosis and cell cycle analysis of HCT116 cells.

A series of novel pteridinone derivatives possessing a hydrazone moiety were synthesized. The general synthetic routes of the target

compounds were described in Scheme 1. Starting from commercially available 2,4-dichloro-5-nitropyrimidine 1, reacted with cyclopentylamine in DCM to yield intermediate 2, which was further reduced by using iron powder and catalytic amounts of concentrated HCl in EtOH/ H_2O to produce intermediate 3. The intermediate 4 was prepared from 3 by condensed with ethyl oxalyl monochloride in acetone. The compound 4 reacted with methyl iodide to afford *N*-alkylated product 5. Subsequently, the intermediate 6 was available via hydrazinolysis of intermediate 5 with 80% hydrazine monohydrate in EtOH at 40 °C.



Scheme 1. General scheme for the synthesis of target compound; Reagents and conditions: (i) Cyclopentylamine, NaHCO_3 , DCM, 25°C , 10 h, 85.0%; (ii) Fe powder, HCl (cat.), EtOH/ H_2O , reflux, 2 h, 73%; (iii) a: Ethyl oxalyl monochloride, K_2CO_3 , acetone, 2 h; b: TEA, EtOH, 100°C , 4 h, 83%; (iv) CH_3I , DCM, rt, 2 h, 97.9%; (v) $\text{NH}_2\text{NH}_2\cdot\text{H}_2\text{O}$, EtOH, 40°C , 2 h; (vi) appropriate aromatic aldehyde, EtOH, 80°C , 5 h, 62.6–83.4%.

Finally, intermediate **6** reacted with appropriate aromatic aldehyde under standard conditions to obtain the target product **L₁–L₃₀** in good or moderate yields.

To evaluate *in vitro* antitumor activities, all synthesized compounds (**L₁–L₃₀**) were investigated against three cancer cell lines including A549 (human lung adenocarcinoma), HCT116 (human colorectal cancer) and PC-3 (human prostate cancer) cells by using MTT assay and BI-2536 was served as the positive control. The antiproliferative results were expressed as half-maximal inhibitory concentration (IC_{50}) values and summarized in Table 1. Most of pteridinone derivatives **L₁–L₃₀** showed moderate to good antiproliferative activities against the different cancer cell lines, which suggested that the combination of 2-amino-5-methyl-5,8-dihydropteridine-6,7-dione framework containing hydrazone moiety exhibited potent synergistic antitumor effect. Preliminary SARs indicated that the introduction of different substituted aromatic rings had a significant influence on activity. Compounds bearing halogen atoms (F, Cl, and Br) substituted phenyl ring showed the significant antiproliferative activity, suggesting that the presence of halogen atoms on phenyl ring was a key factor in the anticancer activity. On the other hand, electron-withdrawing compounds displayed excellent anti-tumor activities in the singular micromolar range against A549 and HCT116 cells (**L₂₂** vs **L₃**). Especially, the most promising compound **L₁₉** exhibited significant potency against A549, HCT116 and PC-3 cells with IC_{50} values of $3.23\ \mu\text{M}$, $4.36\ \mu\text{M}$ and $8.20\ \mu\text{M}$, respectively. But we also observed that compound **L₁₄** shows relatively high activity even though it contains three electron-donating methyl groups. Notably, compounds had significantly improved antiproliferative activity with inserting another identical substituent into the aromatic ring (**L₂₃** vs **L₂₈**, **L₁₄** vs **L₁₆** vs **L₃**). This indicated that incorporating simultaneously favorable substitutions could provide additive effects. The para-methoxy derivative **L₁₈** and the corresponding meta-substituted analog **L₈** showed similar potency against A549, HCT116 and PC-3 cells. However, moving the methoxy group to the *ortho*-position led to a significant reduction in antiproliferative activity (**L₁₇** vs **L₈**, **L₁₈**). Decrease in activity may be due to steric hindrance, resulting in the hydrophobic pocket space collision. These proved that para- and meta-position were more conducive to increasing activity than *ortho*-position. Further studies were performed to examine the effect of shifting the benzene ring group to the aromatic heterocyclic group (**L₁** vs **L₁₂**, **L₁₃**). The results indicating that aromatic heterocyclic modification can preserve anti-proliferative activity.

Overall, the most potent compound **L₁₉** showed promising cytotoxicity against A549, HCT116, and PC-3 cell lines with IC_{50} values of $3.23\ \mu\text{M}$, $4.36\ \mu\text{M}$ and $8.20\ \mu\text{M}$, respectively. **L₁₉** demonstrated the

potential for further development of novel pteridinone derivatives as an effective antitumor agents.

On the basis of the cellular assays, effective compounds were selected to further *in vitro* PLK1% inhibition at $1\ \mu\text{M}$. The results were shown in Fig. 4. Most of compounds inhibited PLK1 kinases with % inhibition values ranging from 49.7% to 75.1%. Parallel to the cellular results, inhibitors bearing electron withdrawing substituent at aromatic ring were found to more potent than others. Among them, **L₁₉** displayed the best inhibitory activity against PLK1 up to 75.1%. These results indicated that pteridinone derivatives bearing hydrazone moiety as new potential anticancer agents for the treatment of human cancers were worthy of further study, and the PLK1 inhibitory activity may increase by structural modifications.

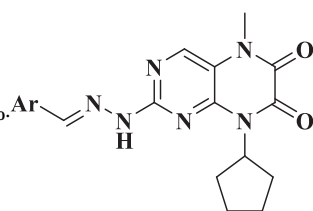
In order to preliminary study the molecular mechanism of action, cell apoptosis analysis was performed on the HCT116 cells treating with $1.0\ \mu\text{M}$, $3.0\ \mu\text{M}$ and $9.0\ \mu\text{M}$ of **L₁₉** for 24 h and using Annexin-V and propidium iodide (PI) double staining by flow cytometry. As shown in Fig. 5, compound **L₁₉** effectively induced apoptosis in a concentration-dependent manner. Compound **L₁₉** proved to induce apoptosis by 38.3% as compared to 18.9% of apoptotic cells in the blank control (Table 2).

Since migration was an important feature of metastatic cancers, the effect of compound **L₁₉** on migration of HCT116 cells was studied by the wound-healing assay. As shown in Fig. 6, the drug concentration of **L₁₉** was $0.3\ \mu\text{M}$ and $3\ \mu\text{M}$, respectively. Compared with the blank control group, the wound healing rate decreased with the prolongation of the action time and **L₁₉** significantly inhibited the wound healing in a concentration-dependent manner.

To investigate the effect of optimal compound **L₁₉** on the mitotic cycle of cell, cell cycle analysis of HCT116 cells treated with **L₁₉** at indicated concentrations (0.3 , 1.0 , $9.0\ \mu\text{M}$) for 24 h, were fixed and performed using Annexin-V and propidium iodide (PI) and the DNA content was analyzed by flow cytometry. The results were compared with HCT116 cells in non-treated control. As shown in Figs. 7.1 and 7.2, treatment of HCT116 cells with **L₁₉** at 0.3 , 1.0 , and $9.0\ \mu\text{M}$ concentrations increased the percentage of G₁-phase cells from 61.81% (as control group) to 62.69%, 65.46%, and 67.2%, respectively. These results certificated that compound **L₁₉** markedly caused G₁-phase arrest in HCT116 cells.

In order to verify the rationality of the design and the mode of action of these compounds and proteins, we used BI-2536/PLK1 co-crystal structure (PDB code: 2RKU) as the docking model, and performed molecular simulation docking of **L₁₉** with PLK1 (Fig. 8). In the protein cavity, compound **L₁₉** (purple) and BI-2536 (green) were nearly

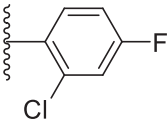
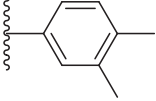
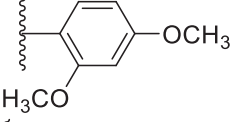
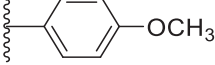
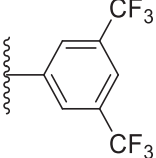
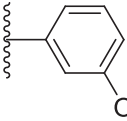
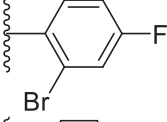
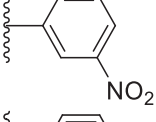
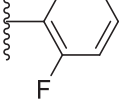
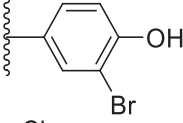
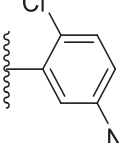
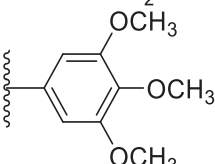
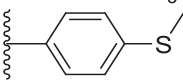
Table 1

Structures and anti-proliferative activities of compound L₁–L₃₀.

Compound	Aromatic ring	IC ₅₀ ^a (μM) ± SD ^b		
		A549	HCT116	PC-3
L ₁		> 100	> 100	48.20 ± 0.2
L ₂		> 100	72.52 ± 0.04	> 100
L ₃		34.50 ± 0.02	> 100	53.59 ± 0.02
L ₄		6.89 ± 0.03	9.81 ± 0.01	8.42 ± 0.04
L ₅		9.41 ± 0.02	9.02 ± 0.02	8.55 ± 0.03
L ₆		84.45 ± 0.04	86.59 ± 0.04	26.59 ± 0.02
L ₇		97.78 ± 0.08	59.30 ± 0.04	85.15 ± 0.02
L ₈		27.43 ± 0.01	45.75 ± 0.02	20.68 ± 0.01
L ₉		40.58 ± 0.02	29.04 ± 0.04	23.61 ± 0.05
L ₁₀		22.92 ± 0.02	27.10 ± 0.04	17.72 ± 0.01
L ₁₁		39.05 ± 0.05	26.36 ± 0.02	17.20 ± 0.01
L ₁₂		> 100	78.74 ± 0.08	72.16 ± 0.04
L ₁₃		> 100	52.59 ± 0.04	75.63 ± 0.08
L ₁₄		12.03 ± 0.01	7.92 ± 0.01	13.88 ± 0.02

(continued on next page)

Table 1 (continued)

Compound	Aromatic ring	IC ₅₀ ^a (μM) ± SD ^b		
		A549	HCT116	PC-3
L ₁₅		10.99 ± 0.02	13.80 ± 0.01	15.18 ± 0.03
L ₁₆		30.18 ± 0.02	62.93 ± 0.04	39.03 ± 0.02
L ₁₇		> 100	> 100	> 100
L ₁₈		> 100	36.11 ± 0.05	26.25 ± 0.02
L ₁₉		3.23 ± 0.04	4.36 ± 0.01	8.20 ± 0.05
L ₂₀		> 100	37.24 ± 0.04	36.30 ± 0.04
L ₂₁		6.59 ± 0.02	8.39 ± 0.01	9.25 ± 0.01
L ₂₂		12.30 ± 0.04	15.23 ± 0.01	20.32 ± 0.03
L ₂₃		31.21 ± 0.1	20.73 ± 0.08	27.59 ± 0.02
L ₂₄		12.84 ± 0.02	17.71 ± 0.02	11.58 ± 0.02
L ₂₅		8.78 ± 0.01	5.61 ± 0.04	9.26 ± 0.02
L ₂₆		18.27 ± 0.02	22.87 ± 0.01	17.50 ± 0.01
L ₂₇		14.10 ± 0.02	9.01 ± 0.03	21.03 ± 0.06

(continued on next page)

Table 1 (continued)

Compound	Aromatic ring	IC ₅₀ ^a (μM) ± SD ^b		
		A549	HCT116	PC-3
L ₂₈		18.31 ± 0.01	19.77 ± 0.01	13.17 ± 0.04
L ₂₉		9.86 ± 0.04	14.03 ± 0.02	16.31 ± 0.02
L ₃₀		12.89 ± 0.08	6.15 ± 0.04	7.18 ± 0.04
BI2536		0.05 ± 0.01	2.03 ± 0.04	0.46 ± 0.01

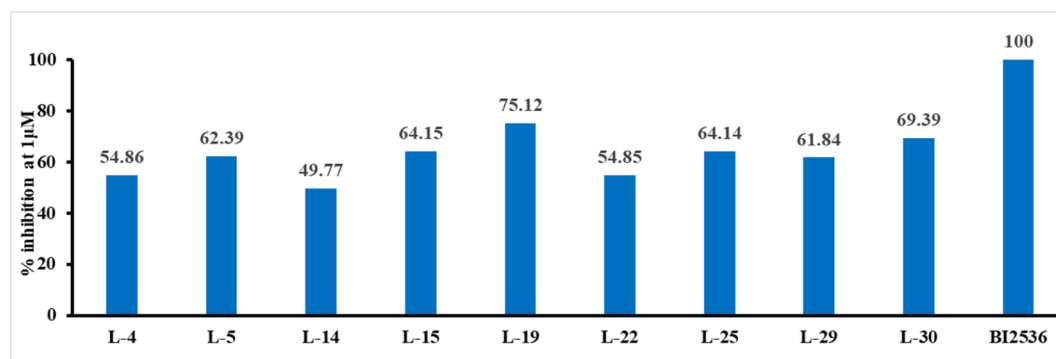
^a Values are the means of at least three independent experiments.^b SD: standard deviation.

Fig 4. Enzymatic activities of the target compounds.

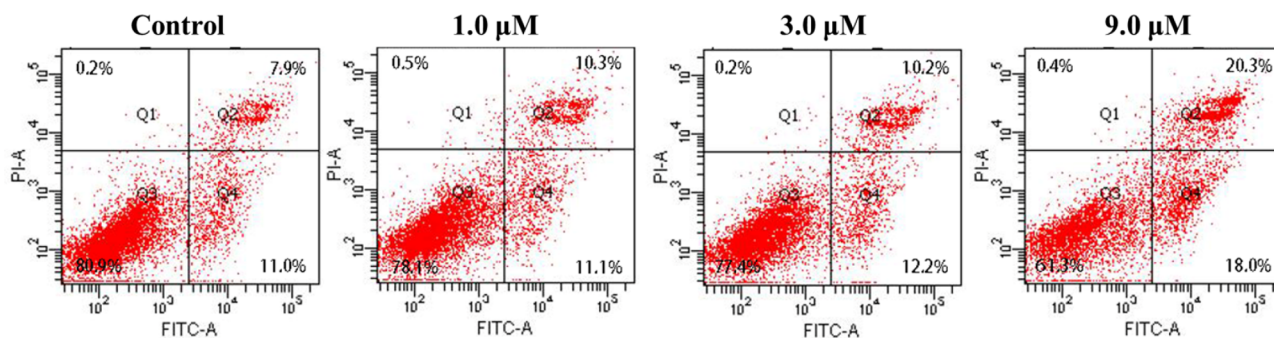
Fig 5. Compound L₁₉ induced apoptosis in HCT-116 cells. Cells were treated with various concentrations of L₁₉ for 24 h and then analyzed the Annexin V-FITC/PI staining test by flow cytometry analysis. Values represent the mean ± S.D, n = 3. P < 0.05 versus the control. The percentage of cells in each part is indicated.

Table 2

Percent of cell death induced by compound L₁₉ (9.0 μM and 0 μM) on HCT116 cells.

Concentrations L ₁₉	Apoptosis (%)			Necrosis (%)
	Total	Early	Late	
9.0 μM	38.3	20.3	18.0	0.4
0 μM	18.9	7.9	11.0	0.2

overlapped, indicating that the modes of binding of the two were basically the same (Fig. 8D). As shown in Fig. 8B, the carbonyls at positions 6 and 7 of the compound L₁₉ formed three hydrogen bonds (blue) with His166, Asp194, and Lys83 via water molecules. At the same time, the bidentate hydrogen bonding of the aminopyrimidine moiety at position 2 was retained, thereby ensuring its inhibitory activity on PLK1. The introduction of hydrazone group did change the position of the aromatic ring and protein (Fig.8D). This may be the reason why the meta- and para-substituted compound on the benzene ring has good

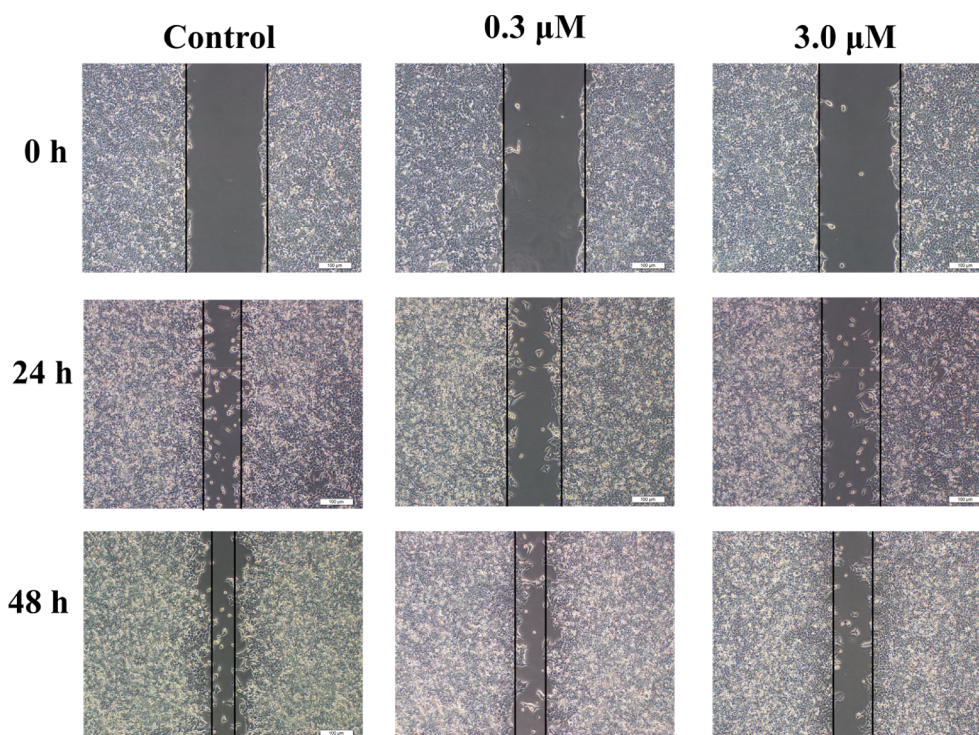


Fig. 6. *In vitro* wound healing assay on HCT116 cells. Phase contrast images were obtained by the treatment of compounds **L**₁₉ at indicated concentrations for 0, 24 and 48 h.

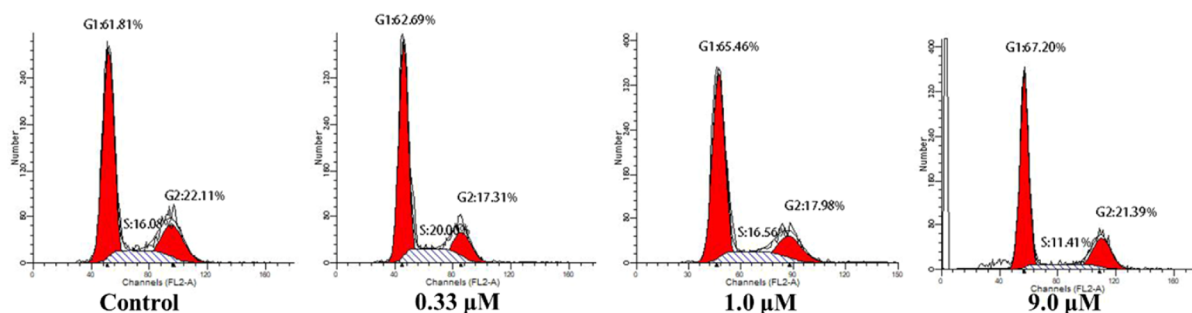


Fig. 7.1. Cycle distribution of HCT116 cell lines. HCT116 cells were treated with different concentrations of **L**₁₉ for 24 h (A: control, B: 0.33 μM, C: 1.0 μM and D: 9.0 μM).

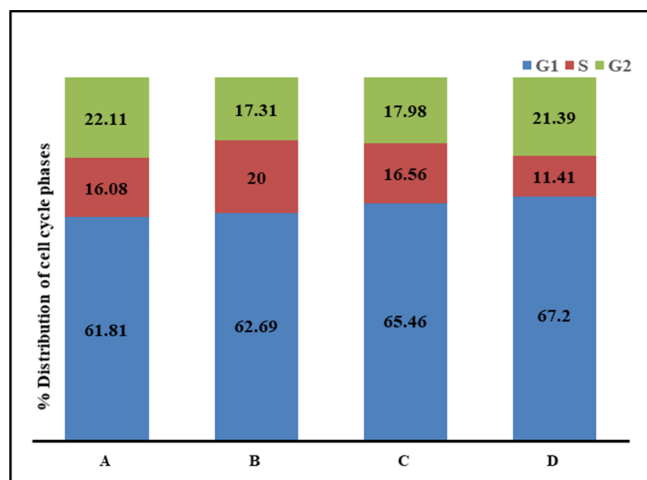


Fig. 7.2. Quantitative analysis of cell cycle distributions; (A) Non-treated cells as control group; (B) treated with **L**₁₉ at 0.33 μM; (C) treated with **L**₁₉ at 1.0 μM; (D) treated with **L**₁₉ at 9.0 μM.

activity. On the other hand, in addition to the Pi-cation interactions of the aromatic ring portion of compound **L**₁₉ with Arg136 and Leu59, the fluorine atom in its trifluoromethyl group forms a hydrogen bond with Arg136, Arg57 and Leu59. This provides unique ideas for follow-up research.

In this study, we have designed and synthesized a series of novel pteridinone derivatives possessing a hydrazone moiety based on the scaffold of PLK1 inhibitor BI-2536. The results of antitumor activity indicated that **L**₁₉ obviously exhibited inhibitory activity against A549, HCT116 and PC-3 cell lines with IC₅₀ values of 3.23 μM, 4.36 μM, and 8.20 μM, respectively. The results of molecular docking and *in vitro* enzymatic studies showed that PLK1 maybe a drug target for compound **L**₁₉. Furthermore, to clarify the antiproliferative activity mechanism, flow cytometry and wound healing tests confirmed that **L**₁₉ induces apoptosis. Finally, the cell cycle analysis of **L**₁₉ by flow cytometry showed that compound **L**₁₉ arrested in the G₁ phase cell cycle. In conclusion, SARs research and pharmacological analysis of novel pteridinone derivatives indicated that **L**₁₉ as a promising candidate is worth of further study.

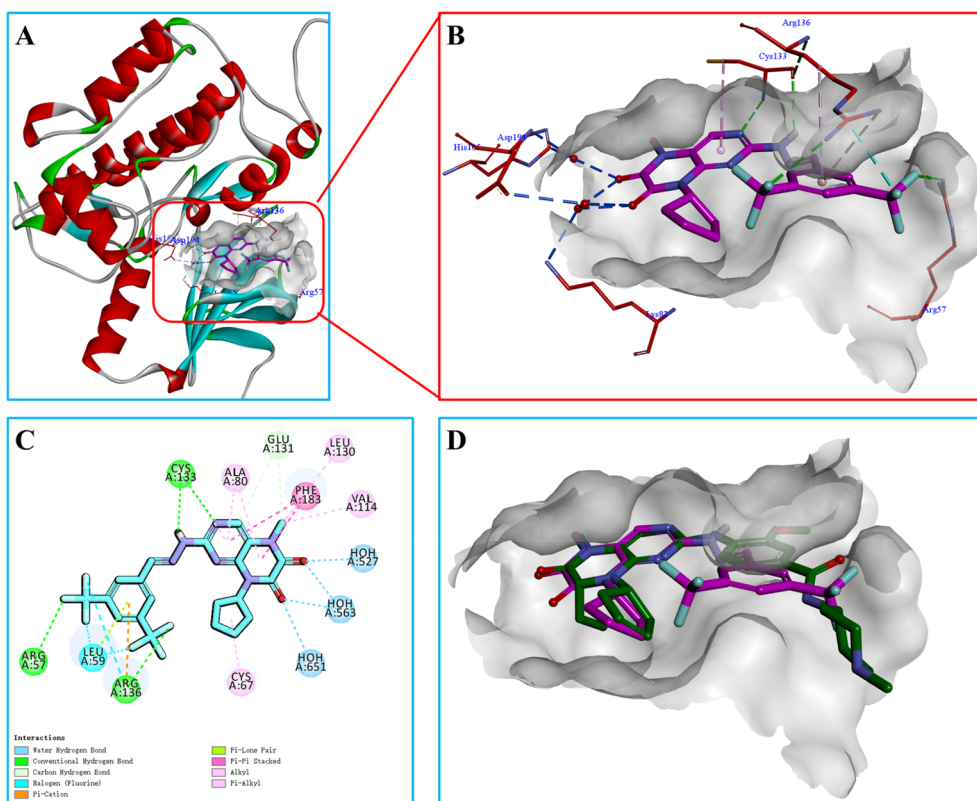


Fig. 8. The binding models of L₁₉ with PLK1. (A, B) Predicted binding conformation for L₁₉ (purple sticks) in the binding site cavity of PLK1 (PDB code: 2RKU). (C) 2D diagram of the interaction between L₁₉ and the binding site cavity of PLK1 (D) L₁₉ overlapping with BI-2536 (green sticks).

Declaration of Competing Interest

The authors declare that they have no known competing financial interests or personal relationships that could have appeared to influence the work reported in this paper.

Acknowledgements

The work was financially supported by the Project funded by China Postdoctoral Science Foundation (2019TQ0215), the Program of Liaoning Revitalization Talents Program (XLYC1808037) and the Doctoral Scientific Research Foundation of Liaoning Province (2020-BS-130).

Appendix A. Supplementary data

Supplementary data to this article can be found online at <https://doi.org/10.1016/j.bmcl.2020.127329>.

References

- Zhang J, Yang PL, Gray NS. *Nat Rev Cancer*. 2009;9:28.
- Siegel RL, Miller KD, Jemal A. *CA Cancer J Clin*. 2016;66:7.
- Peters J-U. *J Med Chem*. 2013;56:8955.
- Combes G, Alharbi I, Braga LG, et al. *Oncogene*. 2017;36:4819.
- De Carcer G, Manning G, Malumbres M, et al. *Cell Cycle*. 2011;10:2255.
- Palmisiano ND, Kasner MT. *Am J Hematol*. 2015;90:1071.
- Strebhardt Klaus. *Nat Rev Drug Discov*. 2010;9:643.
- Xiao D, Yue M, Su H, et al. *Mol Cell*. 2016;64:93.
- Zhang Z, Hou X, Shao C, et al. *Cancer Res*. 2014;74:6635.
- Steehmaier M, Hoffmann M, Baum A, et al. *Curr Biol*. 2007;17:316.
- Rudolph D, Steegmaier M, Hoffmann M, et al. *Clin Cancer Res*. 2009;15:3094.
- Beria I, Bossi RT, Brasca MG, et al. *Bioorg Med Chem Lett*. 2011;21:2969.
- Olmos D, Barker D, Sharma R, et al. *Clin Cancer Res*. 2011;17:3420.
- Nie Z, Feher V, Natala SR, et al. *Bioorg Med Chem Lett*. 2013;23:3662.
- Kothe M, Kohls D, Low S, et al. *Chem Biol Drug Des*. 2007;70:540.
- Hou Y, Zhu L, Li Z, et al. *Eur J Med Chem*. 2019;163:690.
- Rollas Sevim, Gulerman Nehir, Erdeniz Habibe. *IL Farmaco*. 2010;33:96.
- Kucukguzel SG, Oruc EE, Rollas S, Sahin F, Ozbek A. *Eur J Med Chem*. 2002;37:197.
- Wang Y, Yan H, Ma C, Lu D. *Bioorg Med Chem Lett*. 2015;25:4461.
- Wang Y, Zhang G, Hu G, et al. *Eur J Med Chem*. 2016;123:80.
- Liu Z, Wu S, Wang Y, et al. *Eur J Med Chem*. 2014;87:782.